Smad ubiquitination regulatory factor-2 controls gap junction intercellular communication by modulating endocytosis and degradation of connexin43

Tone Aase Fykerud[1], Ane Kjenseth[1], Kay Oliver Schink[1], Solveig Sirnes[1], Jarle Bruun[1], Yasufumi Omori[2], Andreas Brech[1], Edgar Rivedal[1] and Edward Leithe[1,*]

[1]Department of Cancer Prevention, Institute for Cancer Research, the Norwegian Radium Hospital, Oslo University Hospital, Montebello, 0310 Oslo, and Centre for Cancer Biomedicine, Faculty of Medicine, University of Oslo, Oslo, Norway
[2]Department of Molecular and Tumour Pathology, Akita University Graduate School of Medicine, 010-8543 Akita, Japan

*Author for correspondence (eleithe@rr-research.no)

Accepted 8 May 2012
Journal of Cell Science 125, 3966–3976

doi: 10.1242/jcs.093500

Summary

Gap junctions consist of arrays of intercellular channels that enable adjacent cells to communicate both electrically and metabolically. Gap junction channels are made of a family of integral membrane proteins called connexins, of which the best-studied member is connexin43. Gap junctions are dynamic plasma membrane domains, and connexin43 has a high turnover rate in most tissue types. However, the mechanisms involved in the regulation of connexin43 endocytosis and transport to lysosomes are still poorly understood. Here, we demonstrate by live-cell imaging analysis that treatment of cells with 12-O-tetradecanoylphorbol 13-acetate (TPA) induces endocytosis of subdomains of connexin43 gap junctions. The internalized, connexin43-enriched vesicles were found to fuse with early endosomes, which was followed by transport of connexin43 to the lumen of early endosomes. The HECT E3 ubiquitin ligase smad ubiquitination regulatory factor-2 (Smurf2) was found to be recruited to connexin43 gap junctions in response to TPA treatment. Depletion of Smurf2 by small interfering RNA resulted in enhanced levels of connexin43 gap junctions between adjacent cells and increased gap junction intercellular communication. Smurf2 depletion also counteracted the TPA-induced endocytosis and degradation of connexin43. Collectively, these data identify Smurf2 as a novel regulator of connexin43 gap junctions.

Key words: Gap junctions, Connexin43, Smurf2, Ubiquitin, Endocytosis

Introduction

Gap junctions are intercellular plasma membrane domains containing arrays of channels that provide direct exchange of ions and small molecules between adjacent cells. Gap junction channels are composed of tetra-membrane spanning proteins called connexins. The human genome encodes 20 known connexin isoforms, of which connexin43 (Cx43) is the best-studied (Söhl and Willecke, 2003). Gap junctions play important roles in regulation of cell growth and differentiation and in maintenance of tissue homeostasis (Saez et al., 2003). Gap junctions also play fundamental roles in excitable tissues by mediating electrical transmission between cells (Saez et al., 2003). Dysfunctional gap junction intercellular communication has been causally implicated in a variety of diseases, such as deafness, peripheral neuropathies, skin disorders, cataracts and cardiovascular diseases (Saez et al., 2003). There is also significant evidence that aberrant regulation of gap junction intercellular communication is involved in carcinogenesis, and several connexin isoforms, including Cx43, act as tumor suppressors (King and Lampe, 2004; Langlois et al., 2010; McLachlan et al., 2006; Mesnil et al., 2005; Naus and Laird, 2010; Plante et al., 2010; Sirnes et al., 2012; Zhang et al., 2003).

The most rapid form of gap junction channel regulation involves changes in the conductance of single channels or their probability of opening (Saez et al., 2003). Slower regulation of gap junctions is achieved by changing the rate of connexin synthesis, trafficking of connexins to the plasma membrane or assembly of connexins into gap junctions. There is also increasing evidence that gap junction intercellular communication can be regulated at the level of gap junction endocytosis. Gap junctions are highly dynamic plasma membrane domains, and Cx43 has a half-life of 1.5–5 hours in most tissue types (Fallon and Goodenough, 1981; Laird et al., 1991). Cx43 is continually removed from the center of the gap junction plaque by clathrin-mediated endocytosis (Falk et al., 2009; Nickel et al., 2008; Piehl et al., 2007). During endocytosis of gap junctions, both membranes of the junction are internalized into one of the contacting cells, forming a double-membrane vesicle called an annular gap junction or connexosome (Falk et al., 2009; Jordan et al., 2001; Larsen and Hai-Nan, 1978; Leithe et al., 2006a; Leithe et al., 2012; Nickel et al., 2008; Piehl et al., 2007). Following endocytosis, connexins are degraded in lysosomes (Falk et al., 2009; Jordan et al., 2001; Laing et al., 1997; Leithe and Rivedal, 2004b; Leithe et al., 2006a; Naus et al., 1993; Nickel et al., 2008; Piehl et al., 2007; VanSlyke et al., 2000; Vaughan and Lasater, 1992). There is increasing evidence that Cx43 may follow multiple alternative post-endocytic pathways en route to lysosomes. Several studies have shown that Cx43 connexosomes can fuse directly with lysosomes (Murray et al., 1981; Naus et al., 1993; Qin et al., 2003; Vaughan and Lasater, 1990). Other studies have demonstrated that Cx43 connexosomes can be degraded by autophagy (Hesketh et al., 2010; Lichtenstein et al., 2011). Studies

from our laboratory suggest that also a third pathway for post-endocytic sorting of Cx43 to lysosomes exist, in which Cx43 connexosomes undergo a maturation process to form a multivesicular endosome with a single limiting membrane, followed by trafficking of Cx43 to early and late endosomes prior to degradation of Cx43 in lysosomes (Leithe et al., 2006a; Leithe et al., 2009; Sirnes et al., 2008). It is likely that the various pathways for post-endocytic sorting of Cx43 utilize distinct molecular machineries. However, the molecular mechanisms involved in regulation of gap junction endocytosis and sorting of Cx43 to lysosomes are poorly understood.

There is increasing evidence that endocytosis and post-endocytic trafficking of Cx43 is regulated by a complex interplay between Cx43 phosphorylation and ubiquitylation (Kjenseth et al., 2010). Many growth factors, such as epidermal growth factor (EGF), and tumor promoters, including TPA (12-O-tetradecanoylphorbol 13-acetate), inhibit gap junction intercellular communication and induce endocytosis and degradation of Cx43 gap junctions (Asamoto et al., 1991; Berthoud et al., 1993; Kanemitsu and Lau, 1993; Laird, 2005; Lampe, 1994; Lampe et al., 2000; Lampe and Lau, 2000; Rivedal and Opsahl, 2001; Ruch et al., 2001; Warn-Cramer et al., 1998). The TPA-induced phosphorylation, endocytosis and degradation of Cx43 is mediated by protein kinase C (PKC) and the mitogen-activated protein (MAP) kinase pathway (Leithe and Rivedal, 2004b; Rivedal and Leithe, 2005; Sirnes et al., 2009). The TPA-induced phosphorylation of Cx43 is associated with strongly increased Cx43 ubiquitylation (Leithe and Rivedal, 2004b). Ubiquitylation of Cx43 has been suggested to be involved in regulating gap junction endocytosis by recruiting the ubiquitin-binding protein Eps15 (EGF receptor pathway substrate 15) to gap junction plaques (Girão et al., 2009). Ubiquitylation has also been implicated in controlling the trafficking of Cx43 from early endosomes to lysosomes, in a process involving the ubiquitin-binding proteins Hrs (hepatocyte-growth-factor-regulated tyrosine kinase substrate) and Tsg101 (tumor susceptibility gene 101) (Auth et al., 2009; Leithe et al., 2009; Malerød et al., 2011).

The E3 ubiquitin ligases can be classified into three major families: (1) the HECT (homologous to E6-AP carboxy terminal) E3s; (2) the RING (really interesting new gene) E3s; and (3) the U-box E3s (Pickart, 2001). The HECT E3 ubiquitin ligase family comprises 28 members in mammals (Bernassola et al., 2008). The HECT E3 ubiquitin ligases are classified further into subfamilies, among which the Nedd4 (neural precursor cell-expressed developmentally downregulated gene 4) family is the best studied. The Nedd4 family consists of nine members, of which Nedd4-1 is the prototypic member (Ingham et al., 2004). Nedd4-1 has been shown to bind to and catalyze ubiquitylation of Cx43, and is currently the only known E3 ubiquitin ligase involved in regulation of Cx43 gap junctions (Leykauf et al., 2006). Two other relatively well-characterized members of the Nedd4 family are Smurf1 and -2 (smad ubiquitination regulatory factor-1 and -2), which were initially identified as important regulators of the TGF-β (transforming growth factor-β) signaling pathway. Smurf1 and -2 regulate degradation of TGF-β receptor and Smad proteins (Kavsak et al., 2000; Zhang et al., 2001; Zhu et al., 1999). They have also been shown to play important roles in promoting the downregulation of tight junctions during epithelial–mesenchymal transition (EMT), by regulating the degradation of RhoA (Ozdamar et al., 2005). Both Smurf1 and Smurf2 have been shown to be overexpressed in several cancer types and there is increasing evidence that they are causally involved in cancer progression (Fukuchi et al., 2002; Jin et al., 2009). In the present study we identify Smurf2 as a novel regulator of Cx43 gap junctions.

Results

Cx43 is transported to the lumen of early endosomes in response to TPA exposure

Previous studies indicate that exposure of cells to TPA is associated with increased endocytosis of Cx43 gap junctions and subsequent degradation of Cx43 in lysosomes (Asamoto et al., 1991; Leithe et al., 2006a). To obtain a better understanding of the intracellular trafficking of Cx43 in response to TPA treatment, live-cell imaging was performed using a Cx43–EGFP (enhanced green fluorescent protein) chimera. As a model system for studying endocytosis of Cx43 gap junctions, we used IAR20 cells, since these cells express high levels of endogenous Cx43, which under normal growth conditions is organized as gap junctions between adjacent cells (Leithe and Rivedal, 2004a). To verify that the subcellular distribution of Cx43 was not influenced by the EGFP moiety, Cx43–EGFP was transiently transfected into IAR20 cells, and the localization of Cx43–EGFP was compared to that of endogenous Cx43 in fixed cells by confocal microscopy. In accordance with previous studies in other cell types, Cx43–EGFP was found to localize at the plasma membrane and assemble into gap junction plaques in a similar manner as endogenous Cx43 (Fig. 1A) (Jordan et al., 1999; Jordan et al., 2001; Lauf et al., 2002). In order to define early endosomes, cells were co-transfected with Cx43–EGFP and Tomato–EEA1-CT. In agreement with our previous studies on endogenous Cx43 in IAR20 cells, treating cells with TPA in combination with cycloheximide (CHX), to block new protein synthesis, induced a shift in the Cx43–EGFP location from the plasma membrane to intracellular compartments, as determined by confocal microscopy of fixed cells (Fig. 1B). In all subsequent experiments in this study, TPA was co-incubated with CHX. We have previously shown that CHX does not affect the ability of TPA to induce endocytosis and degradation of Cx43 (Leithe and Rivedal, 2004b; Leithe et al., 2006b; Leithe et al., 2009; Rivedal and Leithe, 2005). Importantly, in response to TPA exposure, Cx43–EGFP was found to colocalize with Tomato–EEA1-CT, indicating that Cx43–EGFP was transported to early endosomes (Fig. 1B).

To elucidate the dynamics of Cx43 during gap junction endocytosis and the relationship between Cx43 and early endosomes in live cells, time-lapse fluorescence microscopy was performed. In response to TPA treatment, subdomains of Cx43 gap junctions were observed to bud into one of the adjacent cells, in a similar manner as previously reported during constitutive endocytosis of Cx43 gap junctions in unstimulated cells (Fig. 1C and supplementary material Movie 1) (Falk et al., 2009; Jordan et al., 1999; Jordan et al., 2001; Piehl et al., 2007). Importantly, the internalized Cx43-enriched vesicles were found to undergo fusion with early endosomes. In the course of 60 minutes, the level of Cx43–EGFP-containing gap junctions between adjacent cells was gradually decreased, whereas the intensity of Cx43–EGFP was found to increase at the limiting membrane and the lumen of early endosomes. After 60 minutes of exposure to TPA, the plasma membrane was almost devoid of Cx43–EGFP, whereas the lumen of early endosomes contained

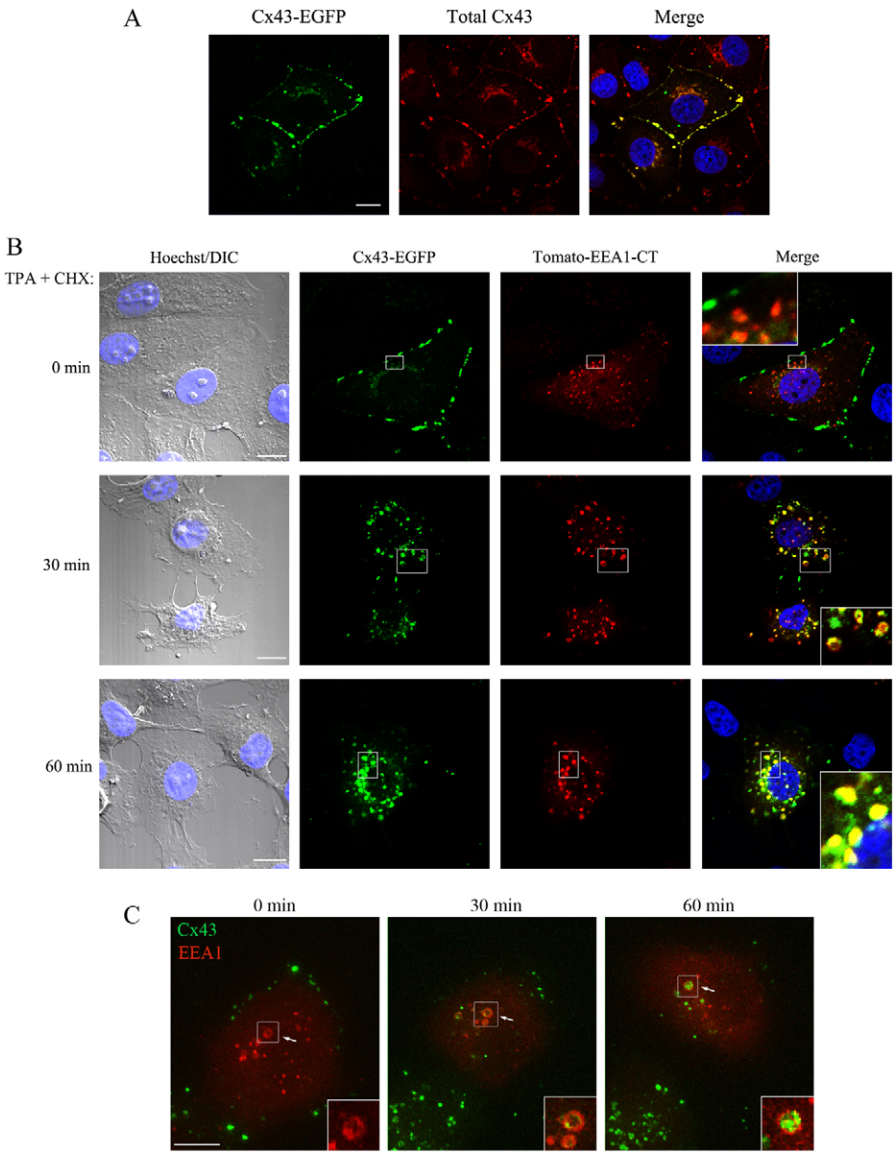

Fig. 1. Cx43 is transported to early endosomes upon TPA and CHX exposure. IAR20 cells were transfected with either Cx43–EGFP plasmids alone (**A**) or in combination with Tomato–EEA1-CT plasmids (**B**,**C**) and analyzed 24 hours after transfection. (A) The cells were fixed and stained with anti-Cx43 antibodies, and Cx43–EGFP and total Cx43 were visualized using immunofluorescence confocal microscopy as indicated. The right panel shows the merged image. Scale bar: 10 µm. (**B**) Cells were left untreated or exposed to TPA (100 ng/ml) in combination with CHX (10 µM) to block new protein synthesis, for 30 or 60 minutes. The cells were then fixed and stained with Hoechst to visualize the nuclei. Cx43–EGFP and Tomato–EEA1-CT were visualized using immunofluorescence confocal microscopy as indicated. The corresponding differential interference contrast (DIC) images are shown. Insets show enlarged views of representative early endosomes. Scale bars: 10 µm. (**C**) IAR20 cells co-expressing Cx43–EGFP and Tomato–EEA1-CT were treated with TPA (100 ng/ml) and CHX (10 µM), and subjected to live cell imaging. Images were collected every minute over a period of 60 minutes. Image capture started 3 minutes after the cells were exposed to TPA and CHX. Insets show enlarged views of representative early endosomes. Arrow indicates an early endosome that is increasingly concentrated with Cx43–EGFP. Scale bar: 10 µm. For the corresponding time-lapse video see supplementary material Movie 1.

Cx43–EGFP (Fig. 1C and supplementary material Movie 1). Notably, Cx43-enriched early endosomes were frequently found to undergo homotypic fusion (supplementary material Movie 1). Collectively, these observations suggest that treating cells with TPA results in internalization of Cx43 gap junctions and subsequent fusion between the internalized Cx43-containing vesicles and early endosomes, followed by transport of Cx43 into the lumen of early endosomes.

Smurf2 is recruited to Cx43 gap junctions in response to TPA exposure

In accordance with previous studies in other cell types, Smurf2 was found to localize both in the cytoplasm and in the nucleus of IAR20 cells, as determined by confocal microscopy (Fig. 2A) (Osmundson et al., 2008). In unstimulated cells, Smurf2 rarely colocalized with Cx43. However, sometimes Smurf2 was found to partly colocalize with Cx43 at gap junctions (supplementary material Fig. S1). Following 15 minutes of TPA exposure, most Cx43 was still organized as gap junctions at the plasma membrane, but the gap junctions often appeared to have started to internalize into one of the adjacent cells. Previous studies have shown that at this time point, Cx43 has lost its Triton X-100 resistance (Leithe et al., 2009; Sirnes et al., 2008). Importantly, in response to treatment of cells with TPA for 15 minutes, Smurf2 was recruited to Cx43 gap junction plaques. Sometimes, a stratification of Smurf2 and Cx43 staining in gap junction regions was observed, with yellow color between, indicative of colocalization between the two proteins (Fig. 2B,C). We have previously shown that gap junctions that are in the process of internalizing into one of the adjacent cells in response to TPA treatment appear to form protrusions into the cytoplasm (Leithe et al., 2009). Such Cx43 gap junction structures were often found to colocalize with Smurf2 (Fig. 2D). Following 30 minutes of TPA exposure, Cx43 was located both at the plasma membrane and in intracellular vesicular structures, in accordance with previous studies (Leithe et al., 2006a). By confocal microscopy, Cx43 was found to partly colocalize with Smurf2 in such intracellular vesicular structures (Fig. 2E). We next investigated whether Smurf2 forms a complex with Cx43, as determined by co-immunoprecipitation. Importantly, Smurf2 was found to

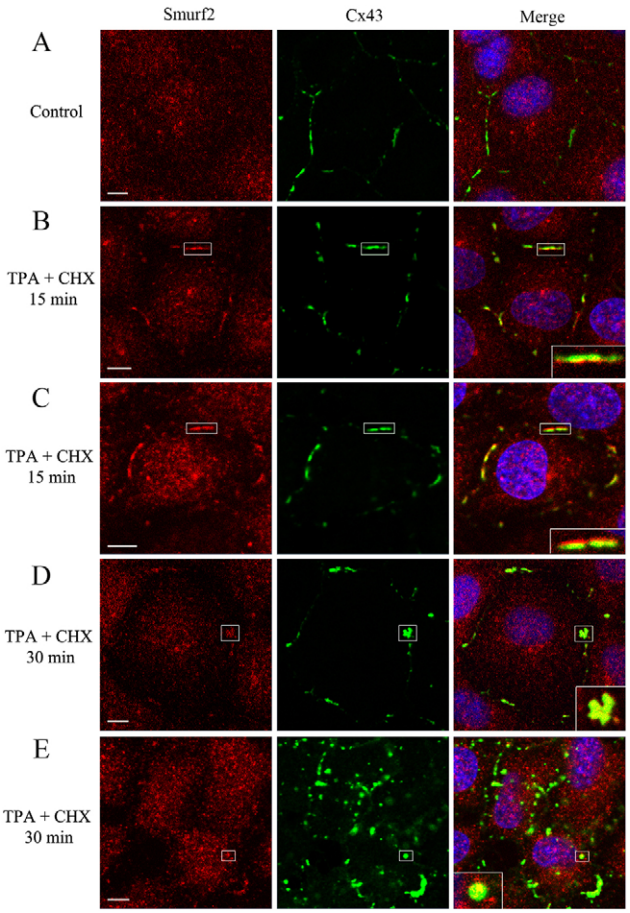

Fig. 2. Smurf2 is recruited to Cx43 gap junctions in response to TPA and CHX treatment. IAR20 cells were left untreated (**A**) or treated with TPA (100 ng/ml) and CHX (10 μM) for 15 minutes (**B**,**C**) or 30 minutes (**D**,**E**). Cells were double-stained with anti-Cx43 and anti-Smurf2 antibodies and visualized using immunofluorescence confocal microscopy. Merged images are shown in the right panels, with yellow indicating co-localization between Cx43 and Smurf2. Insets show enlarged views of representative Cx43 gap junctions or intracellular Cx43-enriched vesicles co-localizing with Smurf2. Scale bars: 5 μm.

co-immunoprecipitate with Cx43 under normal cell growth conditions, and, in line with the confocal microscopy studies, the degree of co-immunoprecipitation between the two proteins was increased in response to TPA treatment (Fig. 3).

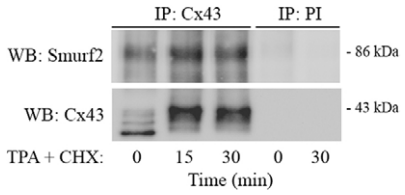

Fig. 3. Smurf2 forms a complex with Cx43. IAR20 cells were left untreated or treated with TPA (100 ng/ml) and CHX (10 μM) for 15 or 30 minutes. Cell extracts were prepared and subjected to immunoprecipitation with anti-Cx43 antibodies or with preimmune serum (PI) as control. Equal amounts of the immunoprecipitates were run on SDS-PAGE followed by western blotting and probing with antibodies against Smurf2 (upper panel). The membrane was stripped and reprobed with anti-Cx43 antibodies (lower panel).

Collectively, these data indicate that Smurf2 is recruited to Cx43 gap junctions in response to TPA treatment.

Depletion of Smurf2 results in increased levels of functional Cx43 gap junctions

To examine the functional importance of Smurf2 in regulation of Cx43 gap junctions, endogenous Smurf2 was depleted by small interfering RNA (siRNA). In these experiments, two distinct siRNA sequences targeting Smurf2 were used (siRNA no. 1 and no. 2), which reduced the Smurf2 protein level by approximately 60% and 70%, respectively, compared to cells transfected with a control siRNA sequence (Fig. 4A). Depletion of Smurf2 did not appear to have major effects on the cell size or morphology (data not shown). Importantly, depletion of Smurf2 caused increased Cx43 protein levels, as determined by western blotting (Fig. 4A). In accordance with the observation that Smurf2 siRNA no. 2 most efficiently depleted Smurf2, this sequence had the strongest effect on the Cx43 protein level, causing an approximate 100% increase, whereas transfection of Smurf2 siRNA no. 1 caused an approximate 50% increase in the Cx43 protein level compared to control cells. Cx43 in IAR20 cells usually migrates in SDS-PAGE gels as three distinct bands, termed Cx43-P0, -P1 and -P2. These bands represent various phosphorylation states of Cx43 and also reflect different subcellular locations of Cx43 (Musil and Goodenough, 1991). The Cx43-P0 band represents newly synthesized Cx43 protein localized in the endoplasmic reticulum, the Golgi apparatus and trans-Golgi network, whereas the Cx43-P1 and -P2 bands represent the Cx43 pool that is organized in gap junctions. Notably, depletion of Smurf2 increased the level of the Cx43-P2 band to a larger extent compared to the Cx43-P0 and -P1 bands (Fig. 4B). In line with these observations, depletion of Smurf2 resulted in enlarged Cx43 gap junctions at the plasma membrane, as determined by confocal microscopy (Fig. 4C). Depletion of Smurf2 did not affect the level of Cx43 in intracellular compartments, in accordance with the observation that the level of Cx43-P0 band on SDS-PAGE was not affected under these conditions. Importantly, depletion of Smurf2 was found to result in increased gap junctional intercellular communication, as determined by quantitative scrape loading (Fig. 4D). Depletion of Smurf2 by transfection with Smurf2 siRNA no. 1 or no. 2 caused an approximate 25% and 40% increase in intercellular communication, respectively, compared with control cells. Taken together, these data indicate that depletion of Smurf2 results in enhanced levels of functional Cx43 gap junctions at the plasma membrane.

Depletion of Smurf2 counteracts endocytosis and degradation of Cx43 gap junctions in response to TPA treatment

Next, we aimed to investigate whether Smurf2 is required for TPA-induced endocytosis of Cx43 gap junctions, as determined by confocal microscopy. In this analysis, the tight junction protein occludin was used as a marker for the cell–cell interphase. As expected, following treatment of control siRNA-transfected IAR20 cells with TPA for 30 minutes, Cx43 was localized both at the plasma membrane and in intracellular vesicles, while after 60 minutes the Cx43 staining was strongly reduced (Fig. 5A). Importantly, cells depleted of Smurf2 had most Cx43 organized as gap junctions between adjacent cells at these time points (Fig. 5A). Quantitative analysis revealed that under normal growth conditions, control and Smurf2-depleted

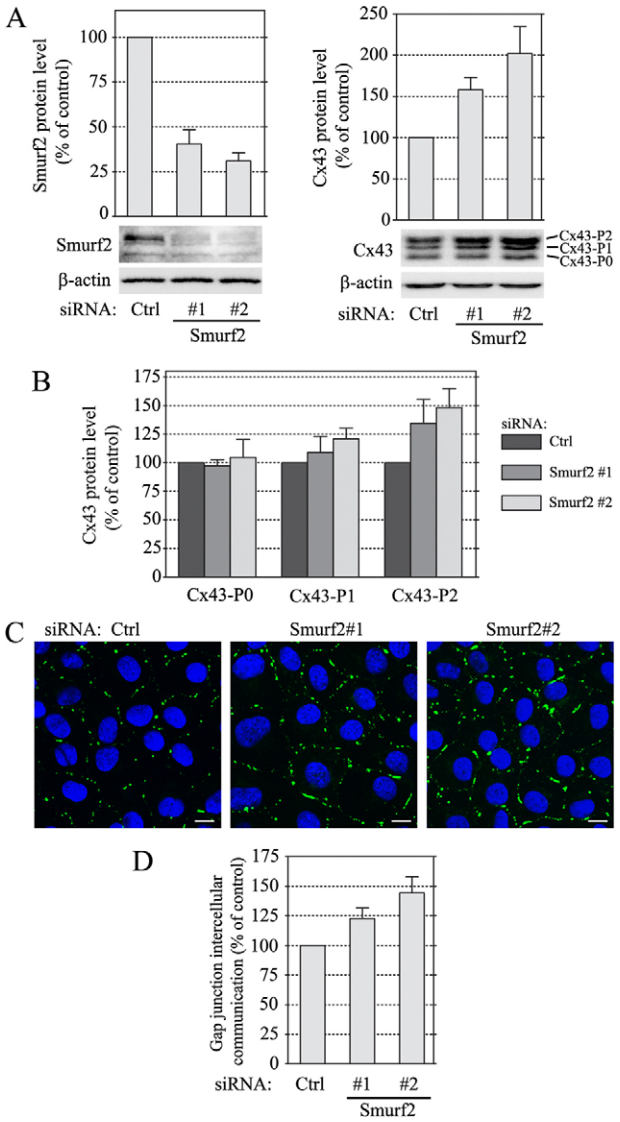

Fig. 4. Smurf2 regulates the level of functional Cx43 gap junctions at the plasma membrane. IAR20 cells were transfected with control siRNA or with either of two different siRNA sequences (no. 1 and no. 2) against Smurf2. (**A**) Cell lysates were prepared 48 hours after transfection, and equal amounts of total cell protein lysates were subjected to SDS-PAGE. Smurf2 and Cx43 were detected by western blotting using antibodies against Smurf2 or Cx43 as indicated. The membranes were stripped and reprobed with antibodies against β-actin as a gel-loading control. The intensities of the Smurf2 and Cx43 bands on western blots were measured using Scion Image and normalized to the β-actin level. Values are the means ± s.d. of three independent experiments. (**B**) The intensities of Cx43 in each band (P0, P1 and P2) in A were measured and normalized to the β-actin level. Values are the means ± s.d. of three independent experiments. (**C**) Cells were fixed 48 hours after transfection, stained with anti-Cx43 antibodies and visualized using immunofluorescence confocal microscopy. Scale bars: 10 μm. (**D**) The level of gap junctional communication was determined by quantitative scrape loading. Values are the means ± s.e.m. of three independent experiments.

cells expressed approximately 50% and 60% of total Cx43 at the plasma membrane, respectively (Fig. 5B). Following 30 minutes of TPA exposure, control siRNA-transfected cells expressed approximately 30% of Cx43 at the plasma membrane, whereas Smurf2-depleted cells still expressed approximately 60% of Cx43

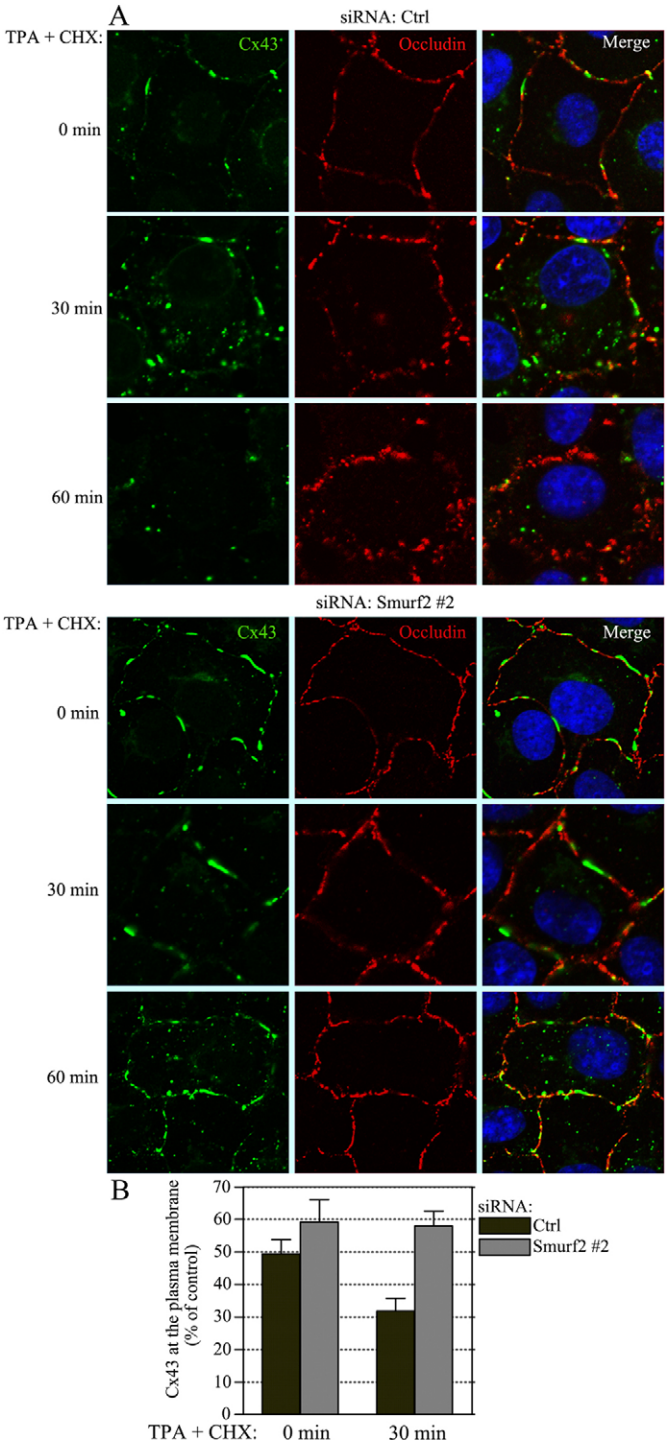

Fig. 5. Smurf2 mediates TPA-induced endocytosis of Cx43 gap junctions. (**A**) IAR20 cells were either transfected with non-targeting siRNA as a control or with Smurf2 siRNA no. 2. After 48 hours of transfection, the cells were treated with TPA (100 ng/ml) and CHX (10 μM) for 30 or 60 minutes as indicated. Cells were fixed, stained with anti-Cx43 and anti-occludin antibodies and visualized using immunofluorescence confocal microscopy. (**B**) The level of Cx43 staining in the cell–cell interface as a percentage of total cellular Cx43 staining in untreated cells and after exposure to TPA and CHX for 30 minutes was determined for siRNA control- and Smurf2 siRNA no. 2-transfected cells. Values are the means ± s.d. of three independent experiments.

at the plasma membrane at this time point (Fig. 5B). These data suggest that Smurf2 is required for efficient endocytosis of Cx43 gap junctions in response to TPA treatment.

We next investigated whether depletion of Smurf2 affected the TPA-induced degradation of Cx43. To this end, cells were transfected with siRNA sequences against Smurf2 or control sequences, and then incubated with TPA and CHX for various time points. In accordance with previous studies, treatment of cells with TPA induced increased levels of the Cx43-P2 band, and reduced level of the Cx43-P0 band as determined by SDS-PAGE (Fig. 6A). This change in the SDS-PAGE band pattern of Cx43 under these conditions is considered to be due to phosphorylation-induced conformational changes of Cx43 (Rivedal and Opsahl, 2001; Sirnes et al., 2009; Solan and Lampe, 2007; Solan and Lampe, 2009). As expected, prolonged treatment of TPA and CHX induced a major loss of Cx43 protein in control siRNA-transfected cells (Fig. 6A,B). Importantly, cells depleted of Smurf2 showed reduced degradation of Cx43 compared to control siRNA-transfected cells (Fig. 6A,B). In accordance with the western blot experiments, treatment of control siRNA-transfected cells with TPA and CHX for 1.5 hours resulted in almost complete loss of Cx43 gap junctions, as determined by confocal microscopy (Fig. 6C). In contrast, cells depleted of Smurf2 expressed considerable amounts of Cx43 organized as gap junctions between adjacent cells, as well as some Cx43 in intracellular vesicles, at this time point (Fig. 6C). We have previously shown that after 3 hours of TPA and CHX treatment, the remaining Cx43 protein is partly relocalized to the plasma membrane, since PKC at this time point is downregulated (Leithe et al., 2003; Leithe et al., 2009). In accordance with this observation, treatment of control siRNA-transfected cells with TPA and CHX for 3 hours resulted in strongly reduced Cx43 expression, except for the presence of some Cx43 organized as small gap junctions at the plasma membrane. Also at this time point, cells depleted of Smurf2 showed more Cx43 staining compared to the control siRNA-transfected cells, most of which was located at the plasma membrane in gap junction plaques (Fig. 6C). Altogether, these data indicate that Smurf2 is required for efficient degradation of Cx43 in response to TPA treatment.

Role of Smurf2 in regulation of Cx43 ubiquitylation

The above experiments suggest that Smurf2 is involved in mediating endocytosis and degradation of Cx43. Smurf2 could affect Cx43 directly by regulating Cx43 ubiquitylation, or it could affect Cx43 indirectly by catalyzing ubiquitylation and degradation of other proteins that control endocytosis and degradation of gap junctions. To investigate whether Smurf2 is involved in regulating Cx43 ubiquitylation, we examined whether depletion of Smurf2 affected the ubiquitylation status of Cx43 under normal growth conditions and in response to TPA treatment. In accordance with previous studies, ubiquitylated Cx43 was detected as a smear containing three distinct bands with approximate molecular mass of 51, 59 and 66 kDa, representing Cx43 conjugated to one, two and three ubiquitin moieties, respectively. Interestingly, there was no major change in the ubiquitylation level of Cx43 in Smurf2-depleted cells compared to control cells (Fig. 7A). As expected, following TPA treatment for 15 minutes, the control siRNA-transfected cells showed increased levels of ubiquitylated Cx43 compared to untreated cells (Fig. 7A). Depletion of Smurf2 did not appear to

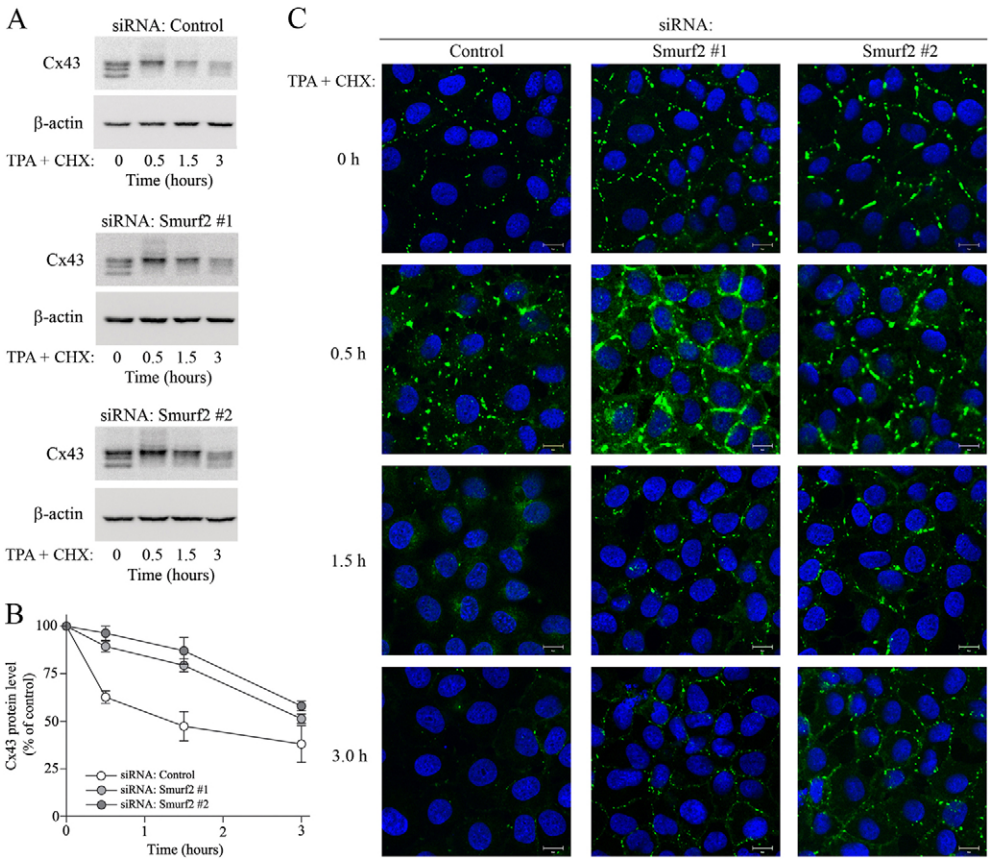

Fig. 6. Smurf2 mediates TPA-induced degradation of Cx43. (**A**) IAR20 cells were either transfected with non-targeting siRNA as a control or with two different siRNA sequences against Smurf2 (siRNA no. 1 and no. 2). After 48 hours of transfection, the cells were treated with TPA (100 ng/ml) and CHX (10 μM) for the given periods of time. Cell lysates were then prepared, and equal amounts of total cell protein were subjected to SDS-PAGE. Cx43 was detected by western blotting, using anti-Cx43 antibodies. The blots were stripped and reprobed with anti-β-actin antibodies. (**B**) The intensities of the Cx43 bands shown in A were quantified and normalized to the level of β-actin. Values are the means ± s.d. of three independent experiments. (**C**) IAR20 cells were either transfected with non-targeting siRNA as a control or with two different siRNA sequences against Smurf2 (siRNA no. 1 and no. 2). After 48 hours of transfection, the cells were treated with TPA (100 ng/ml) and CHX (10 μM) for the given periods of time. Cells were fixed, stained with anti-Cx43 antibodies and visualized using immunofluorescence confocal microscopy. Scale bars: 10 μm.

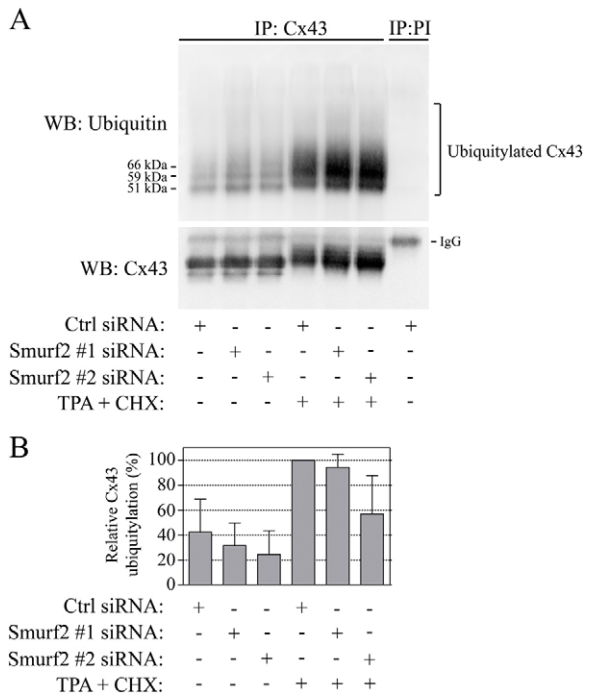

Fig. 7. Effect of Smurf2 depletion on Cx43 ubiquitylation. (**A**) IAR20 cells were transfected with control siRNA or with siRNA against Smurf2 (siRNA no. 1 and no. 2) as indicated. After 48 hours the cells were left untreated or treated with TPA (100 ng/ml) and CHX (10 μM) for 15 minutes. Cells were then subjected to immunoprecipitation with anti-Cx43 antibodies or with preimmune serum (PI) as control. Equal amounts of immunoprecipitates were subjected to SDS-PAGE, and ubiquitin was detected by western blotting using anti-ubiquitin antibodies (upper panel). The blot was stripped and reprobed with anti-Cx43 antibodies (lower panel). (**B**) Quantification of ubiquitylated Cx43 based on the immunoprecipitation study in A. IAR20 cells were transfected with control siRNA or with siRNA against Smurf2 and treated with TPA and CHX as described in A. For each treatment, the level of ubiquitin immunoreactivity was normalized to the level of Cx43 immunoreactivity. Values are the means ± s.d. of three independent experiments relative to control siRNA-transfected cells treated with TPA and CHX.

have major effects on the TPA-induced ubiquitylation of Cx43. Notably, cells depleted of Smurf2 appeared to have a higher level of ubiquitylated Cx43 compared to control siRNA-transfected cells, but this increase is likely to reflect the increase in the total Cx43 protein level under these conditions. In line with this notion, quantification of the level of ubiquitylated Cx43 relative to non-ubiquitylated Cx43 suggested that there was not an increase in Cx43 ubiquitylation in Smurf2-depleted cells (Fig. 7B). Instead there was a tendency towards reduced Cx43 ubiquitylation following knockdown of Smurf2 in both unstimulated and TPA-exposed cells.

Discussion

In this study, we aimed to obtain a better understanding of the mechanisms involved in the endocytosis and degradation of Cx43 gap junctions. Live-cell imaging analysis revealed that exposure of cells to TPA causes endocytosis of fragments of Cx43 gap junctions, and that the internalized Cx43-containing vesicles are able to fuse with early endosomes, which is followed by transport of Cx43 to the lumen of early endosomes. Smurf2 was recruited to Cx43 gap junctions under these conditions, and was required for efficient endocytosis and degradation of Cx43. Moreover, depletion of Smurf2 resulted in enhanced levels of Cx43 gap junctions at the plasma membrane and increased gap junctional intercellular communication. Collectively, these data suggest that Smurf2 controls the level of functional Cx43 gap junctions between adjacent cells by modulating Cx43 endocytosis and degradation.

Previous studies have shown that Cx43 is ubiquitylated in response to TPA treatment, which is associated with increased endocytosis of gap junctions and subsequent degradation of Cx43 in lysosomes (Leithe and Rivedal, 2004b; Leithe et al., 2009). Nedd4-1 has been found to bind to Cx43 and to be involved in the regulation of Cx43 ubiquitylation and gap junction endocytosis (Girão et al., 2009; Leykauf et al., 2006). Here, we have identified another member of the Nedd4 E3 ubiquitin ligase family, Smurf2, as an important regulator of Cx43 gap junctions. The finding that Cx43 is controlled by more than one E3 ubiquitin ligase is in line with previous studies on other proteins, showing that the turnover of a given protein can be regulated by several E3 ubiquitin ligases. For instance, the TGF-β receptor has been shown to be regulated by multiple members of the HECT E3 ubiquitin ligase family (Inoue and Imamura, 2008). Our data suggest that Cx43 is efficiently ubiquitylated although Smurf2 is depleted, both in unstimulated cells and in response to TPA treatment. These observations suggest that also other E3 ubiquitin ligases are involved, and raise the possibility that Smurf2 might regulate Cx43 gap junction endocytosis indirectly via a yet unknown Cx43-binding protein. In this context, it is interesting to note that although Smurf2 has a key role in controlling endocytosis of the TGF-β receptor, Smurf2 does not directly ubiquitylate the receptor. Instead, Smurf2 regulates endocytosis and degradation of the receptor indirectly by ubiquitylation of the adaptor protein Smad7 (Kavsak et al., 2000). The Smurf2-mediated ubiquitylation of Smad7 results in internalization and degradation of the TGF-β-receptor–Smad7 complex. Smurf1 and Smurf2 also regulate tight junctions indirectly by inducing ubiquitylation and degradation of RhoA (Ozdamar et al., 2005). The precise molecular mechanism by which Smurf2 regulates endocytosis of Cx43 gap junctions remains an important subject for future studies. Smurf1 and Smurf2 have many target proteins in common, but have also been shown to regulate different substrates (Osmundson et al., 2009). As determined by western blotting, IAR20 cells expressed relatively low levels of Smurf1 (data not shown). Thus, the role of Smurf1 in Cx43 endocytosis was not investigated further in the present study, and more work is required to elucidate whether Smurf1 has an equally important role in the regulation of Cx43 gap junctions as Smurf2.

There is increasing evidence that multiple pathways may be involved in endocytosis of Cx43 gap junctions and post-endocytic trafficking of Cx43 to lysosomes (Leithe et al., 2012). Several studies indicate that Cx43 connexosomes are able to fuse directly with lysosomes (Murray et al., 1981; Naus et al., 1993; Qin et al., 2003; Vaughan and Lasater, 1990). However, there is increasing evidence that Cx43 may also follow alternative pathways en route to its degradation in lysosomes. Previous studies from our laboratory suggest that in response to TPA treatment, Cx43 connexosomes are able to undergo a maturation process to form a Cx43-enriched multivesicular endosome with a single limiting membrane (Leithe et al., 2006a; Leithe et al., 2009). This morphological transformation

of the connexosome was suggested to be accompanied by trafficking of Cx43 to early endosomes, prior to its transport to lysosomes. Our proposed model for endocytosis of Cx43 gap junctions implies that the connexons organized in gap junctions undock during the endocytic process, and that the Cx43 pool residing in early endosomes thus represents undocked connexons. This notion is in line with our previous studies showing that the Triton X-100 resistance of Cx43 is lost shortly after TPA exposure (Leithe et al., 2009; Sirnes et al., 2008). Possibly, the TPA-induced phosphorylation of Cx43 may cause a conformational shift in the Cx43 gap junction channel that triggers undocking of the connexons. The early endosome is a major sorting station for internalized plasma membrane proteins, and following their entry to early endosomes, endocytosed proteins can be trafficked further downstream to late endosomes and lysosomes, to the trans-Golgi network, or be recycled to the plasma membrane (Gould and Lippincott-Schwartz, 2009). Thus, obtaining a clearer understanding of the role of early endosomes in the post-endocytic sorting of Cx43 may have important implications for understanding how the level of gap junction intercellular communication is regulated. In line with this notion, we have previously reported that depletion of the ubiquitin-binding proteins Hrs or Tsg101 partly counteracts TPA-induced trafficking of Cx43 from early endosomes to lysosomes, which affects the level of functional Cx43 gap junctions at the plasma membrane (Leithe et al., 2009). Based on immuno-electron and confocal microscopy studies of fixed cells, we have previously hypothesized that the transport of Cx43 to early endosomes could be due to direct fusion between internalized Cx43-enriched vesicles and early endosomes (Leithe et al., 2006a; Leithe et al., 2009). In the present study we investigated the intracellular sorting pathway followed by Cx43–EGFP in response to TPA exposure using live-cell imaging analysis. We found that TPA treatment induces endocytosis of subdomains of Cx43 gap junctions, and that the resulting Cx43-enriched vesicles were able to fuse with early endosomes. Prolonged exposure to TPA was found to cause a nearly complete loss of Cx43 gap junctions at the plasma membrane, which was associated with increased localization of Cx43 in the lumen of early endosomes. To the best of our knowledge, these data represent the first live-cell imaging evidence that Cx43 is trafficked to the lumen of early endosomes following endocytosis of gap junctions.

During gap junction endocytosis, both membranes of the plaque are internalized into one of the adjacent cells. As determined by confocal microscopy, Smurf2 sometimes appeared to localize to only one side of gap junction plaques in response to TPA treatment. One possible explanation for this asymmetric localization is that Smurf2 is recruited to the plaque only in the cell in which the plaque is internalized. This would be in line with the finding that Smurf2 is required for efficient endocytosis of Cx43 gap junctions in response to TPA treatment. The finding that Smurf2 was often found to localize on only one side of the plaque is also in accordance with the notion that Smurf2 could regulate ubiquitylation of a yet unknown Cx43 binding protein that is involved in the regulation of gap junction endocytosis.

The data obtained in the present study indicate that Smurf2 plays an important role in mediating the trafficking of Cx43 from the plasma membrane to early endosomes and lysosomes in response to exposure of TPA. It is, however, important to realize that also other trafficking pathways could be involved in the TPA-induced degradation of Cx43. The increased staining of Cx43 in intracellular compartments and enhanced Cx43 degradation in response to TPA treatment may involve alterations in the secretory pathway, as Cx43 has been shown to be able to be transported to lysosomes directly from early secretory compartments (Qin et al., 2003). It is also possible that TPA may induce endocytosis of Cx43 connexons at the plasma membrane not organized in gap junctions. Recent studies have also demonstrated that Cx43 connexosomes can undergo degradation by autophagy (Hesketh et al., 2010; Lichtenstein et al., 2011). Increasing evidence suggests that ubiquitylation may be involved in targeting proteins for degradation by autophagy (Clague and Urbé, 2010). Interestingly, a recent study by Bejarano et al. indicates that Nedd4-mediated ubiquitylation of Cx43 is involved in autophagy-dependent degradation of Cx43 (Bejarano et al., 2012).

There is significant evidence that loss of gap junction intercellular communication is causally involved in carcinogenesis, and Cx43 has been shown to act as a tumor suppressor in various tissue types (Mesnil et al., 2005; Naus and Laird, 2010). Cancer development is associated with either downregulation of Cx43 expression or relocalization of Cx43 from the plasma membrane to intracellular compartments (Leithe et al., 2006b). Several members of the Nedd4 family, including Smurf2, are frequently overexpressed in tumors and have been proposed to act as proto-oncogenes (Bernassola et al., 2008; Ingham et al., 2004). The finding that Smurf2 regulates endocytosis and degradation of Cx43 raises the possibility that overexpression of Smurf2 could contribute to the relocalization of Cx43 from the plasma membrane to intracellular compartments and downregulation of Cx43 in tumors. Smurf1 and Smurf2 have been shown to play important roles in promoting downregulation of tight junctions during EMT (Ozdamar et al., 2005). Smurf2 overexpression correlates with increased metastasis and poor prognosis in patients with esophageal squamous cell carcinoma (Fukuchi et al., 2002). Overexpression of Smurf2 has also been found to be associated with more aggressive metastasic properties of breast cancers (Jin et al., 2009). Importantly, loss of Cx43 expression in breast cancer cells has been shown to be associated with EMT and enhanced migration and invasion (Langlois et al., 2010; McLachlan et al., 2006; Plante et al., 2010). The present study establishes a direct functional link between Smurf2 and Cx43 gap junctions, and may have important implications for understanding the molecular basis underlying the loss of Cx43 gap junctions during EMT.

Materials and Methods

Cell culture

The rat liver epithelial cell line IAR20, originally isolated from normal inbred BD-IV rats was obtained from the International Agency for Research on Cancer (Lyon, France) (Montesano et al., 1975). Cells were grown in Dulbecco's modified Eagle's medium (DMEM) supplemented with 10% (v/v) fetal bovine serum (FBS; Gibco BRL Life Technologies, Inchinnan, UK). The growth medium was replaced with DMEM supplemented with 1% (v/v) FBS 24 hours prior to experiments.

Reagents and antibodies

TPA, CHX, Lucifer yellow and chlordane were obtained from Sigma (St Louis, MO). Anti-Cx43 antibodies were obtained by injecting rabbits with a synthetic peptide consisting of the 20 C-terminal amino acids of Cx43 (Rivedal et al., 1996). Mouse anti-Cx43 antibodies were from Chemicon International, Inc. (Temecula, CA). Rabbit anti-Smurf2 antibodies were obtained from Santa Cruz (Berkeley, CA). Mouse anti-occludin was from Invitrogen. Mouse anti-EEA1 antibodies were from BD transduction laboratories (San Diego, CA). Mouse P4D1 anti-ubiquitin antibodies were obtained from Covance (Berkeley, CA). Mouse anti-actin antibodies were from Sigma. Alexa-Fluor-488-conjugated goat anti-rabbit IgG

and Alexa-Fluor-594-conjugated goat anti-mouse IgG were from Molecular Probes (Eugene, OR). Horseradish peroxidase-conjugated goat anti-rabbit IgG secondary antibodies were from Bio-Rad (Hercules, CA). Horseradish peroxidase-conjugated donkey anti-mouse IgG antibodies were obtained from Jackson ImmunoResearch Laboratories Inc. (West Grove, PA).

DNA and siRNA transfection

The expression plasmid encoding Cx43–EGFP was a kind gift from Klaus Willecke (University of Bonn, Germany). The Tomato–EEA1-CT construct, made by recombining pDest-Tomato and pEntr-EEA1-CT, was kindly provided by Harald Stenmark (The Norwegian Radium Hospital, Oslo, Norway). IAR20 cells were transfected with DNA 24 hours after seeding, using Lipofectamine 2000 (Invitrogen), according to the manufacturer's procedure. Prior to transfection, the medium was replaced with serum-free DMEM. Five hours after transfection, the medium was replaced with DMEM containing 10% (v/v) FBS. Cells were analyzed 24 hours after transfection. The siRNA oligos targeted against *Smurf2* were obtained from Invitrogen [Stealth Select RNAi SMURF2RSS314469 (sequence 1) and SMURF2RSS314470 (sequence 2)], and had the following sequences: 5′-ACAACAGGGUCAGGUAUAUUUCUUA-3′ (sequence 1) and 5′-GAGAUGAUAUCUACACGUUACAGAU-3′ (sequence 2). As siRNA control construct, Stealth RNAi Negative Control (Medium GC; Invitrogen) was used. siRNA was transfected into cells using Lipofectamine 2000 (Invitrogen) at a final concentration of 80 nM, according to the manufacturer's procedure. The growth medium was replaced with DMEM supplemented with 1% (v/v) FBS 24 hours after transfection. The cells were assayed 48 hours after transfection.

Quantitative scrape loading

Determination of gap junctional communication by quantitative scrape loading was performed as previously described (el Fouly et al., 1987; Opsahl and Rivedal, 2000). Briefly, confluent IAR20 cells grown in 35 mm Petri dishes were washed twice with PBS and added 0.05% (w/v) Lucifer Yellow (Sigma) dissolved in PBS without Ca^{2+} and Mg^{2+}. The monolayer was then cut with a surgical scalpel. After 3 minutes, the Lucifer Yellow solution was removed, the dishes rinsed four times with PBS, fixed in 4% formaldehyde in PBS and mounted with a glass coverslip. Digital monochrome images were acquired by a COHU 4912 CCD camera (COHU Inc., San Diego, CA, USA) and a Scion LG-3 frame grabber card (Scion Corporation, Frederick, MD). The levels of gap junctional intercellular communications were determined as the relative area of dye coupled cells, using NIH Image software. Exposing the cells to 30 µM chlordane for 1 hour results in a complete inhibition of gap junctional intercellular communication. Thus, the fluorescent cells following such exposure have obtained the dye directly through the scrape process and were used to define zero GJIC. Values are the means ± s.e.m. of three independent experiments.

Immunostaining and confocal laser-scanning microscopy

IAR20 cells grown in monolayer were fixed with 4% formaldehyde in PBS for 30 minutes at room temperature, rinsed in PBS and permeabilized with 0.1% Triton X-100 for 30 minutes. The cells were then rinsed twice in PBS and incubated with PBS containing 5% (w/v) dry milk and 0.1% Tween for 30 minutes. The cells were incubated with primary antibodies for 1 hour or overnight, washed with PBS and incubated with Alexa-Fluor-488- and/or Alexa-Fluor-594-conjugated secondary antibodies for 1 hour. The cells were then rinsed in PBS and the nuclei were stained with Hoechst 33342 prior to mounting with Mowiol. The cells were analyzed with a LSM 710 META confocal microscope (Carl Zeiss) equipped with a Plan Apochromat 63× 1.4 NA oil immersion objective (Carl Zeiss). Images were acquired with the ZEN 2009 edition software and processed with Adobe Photoshop CS4. The level of Cx43 staining in the cell–cell interface as a percentage of the total cellular Cx43 staining in the same focal plane was quantified using ImageJ software. The cell–cell boundaries were defined based on occludin staining. The plasma membrane-associated Cx43 was then measured by integrating the signal intensity within a region along the cell–cell borders with a constant width. First, a line was drawn to define the cell–cell boundaries, based on occludin staining (red fluorescence; supplementary material Fig. S2A,B). The line was then transferred 15 pixels into the cell (marked 'a' in supplementary material Fig S2C). A second line (marked 'b') was then created 30 pixels outwards from line 'a'. The Cx43 staining localized between lines 'a' and 'b' was defined as Cx43 localized at or in close proximity to the plasma membrane (supplementary material Fig. S2D). The occludin staining (red) and DNA staining (blue) were then excluded from the image and the integrated density of the Cx43 staining (green) was determined between lines 'a' and 'b' (defines Cx43 at the plasma membrane) and inside line 'a' (defines Cx43 in the cytoplasm) after conversion to a 16-bit grayscale image.

Live-cell imaging

IAR20 cells were seeded in Lab-Tek eight-well chamber slides with coverslip bottom (Nunc). The cells were co-transfected with Cx43–EGFP and Tomato–EEA1-CT 24 hours after seeding. Live-cell imaging was performed 24 hours after transfection using a Deltavision microscope (Applied Precision) equipped with Elite TruLight Illumination System, a CoolSNAP HQ2camera and a 60× Plan Apochromat (1.42 NA) lens. For temperature control during live observation, the microscope was kept at 37℃ in a temperature-controlled room. Prior to image capture, growth medium was replaced with medium containing TPA (100 ng/ml) and CHX (10 µM). Image capture started three minutes after adding TPA and CHX, and images were taken every minute over a period of 60 minutes. Time-lapse images were acquired as 18 z-sections, 0.6 µm apart, and deconvolved using the softWoRx software (Applied Precision).

SDS-PAGE and western blotting

IAR20 cells grown in 35-mm Petri dishes were washed with PBS and scraped in 300 µl sodium dodecyl sulfate (SDS) electrophoresis sample buffer (10 mM Tris, pH 6.8, 15% w/v glycerol, 3% w/v SDS, 0.01% w/v Bromophenol Blue and 5% v/v 2-mercaptoethanol). The cell lysates were sonicated and heated for 5 minutes at 95℃. Samples were separated by 8% SDS-PAGE and transferred to nitrocellulose membranes as described (Rivedal et al., 1996). The membranes were developed with chemiluminescence (Lumiglo, Millipore) or Super Signal West Femto Maximum Sensitivity Substrate (Pierce) and imaged on a Kodak Image Station 4000R. The intensity was quantified using Carestream software. Alternatively, the Bio-Rad image station was used for imaging, and bands were quantified using Image Lab software.

Crosslinking of anti-Cx43 antibodies to protein-A–Sepharose beads and immunoprecipitation

In order to covalently link anti-Cx43 antibodies to protein-A–Sepharose beads, the beads were left to swell in immunoprecipitation coupling buffer (dH_2O, 100 mM $NaHCO_3$, 50 mM NaCl, 1 mM PMSF, pH 8.3) for 30 minutes and then mixed with anti-Cx43 antibodies and incubated for 1 hour with continuous end-over-end gentle rotation. The beads were washed twice with 10 volumes of 0.2 M borate buffer (pH 9). Dimethyl pimelimidate dihydrochloride (DMP) was added to a final concentration of 2 mM, and the mix was incubated for 30 minutes. The crosslinking reaction was terminated by washing the beads twice in 10 volumes of 0.2 M ethanolamine (pH 8). The beads were left in the last wash for 2 hours with gentle mixing. The ethanolamine was discarded and the beads were resuspended in the original volume of ice-cold PBS containing 1 mM phenylmethylsulfonyl fluoride (PMSF). IAR20 cells grown in 100-mm Petri dishes were washed once with ice-cold PBS and added lysis buffer [PBS, 10% glycerol, 0.25% sodium deoxycholate, 0.45% sodium lauroyl sarcosine, 20 mM *N*-ethylmaleimide, protease and phosphatase inhibitor cocktails (Sigma), and 2 mM EDTA] for 5 minutes on ice. The lysates were precleaned by incubation with protein-A–Sepharose beads (Invitrogen) at 4℃ for 30 minutes with shaking. Beads were pelleted by centrifugation at 7000 rpm for 5 minutes at 4℃, and the supernatant was collected. To each sample, equal amounts of anti-Cx43 covalently linked to protein-A–Sepharose beads were added. Preimmune serum from the same animal was used as negative control. The reaction mixture was incubated at 4℃ for 2 hours with shaking. The pellet was collected by centrifugation at 5000 rpm for 5 minutes at 4℃ and washed five times with ice-cold lysis buffer containing 20 mM *N*-ethylmaleimide. After the final wash, the pellet was resuspended in 15 µl western sample buffer and heated to 95℃ for 5 minutes. The samples were centrifuged at 13,000 rpm and the supernatant was subjected to protein separation by 8% SDS-PAGE. Western blot analysis was performed as described above.

Acknowledgements

We are grateful to Zeremariam Yohannes, Mette Eknæs, Merete Hektoen and Marianne Smestad for excellent technical assistance, to Klaus Willecke (University of Bonn, Germany) for kindly providing the Cx43-EGFP plasmid, and to Harald Stenmark (Norwegian Radium Hospital, Oslo, Norway) for kindly providing the Tomato-EEA1-CT plasmid and for helpful discussions. We also thank the confocal microscopy core facility at the Institute for Cancer Research, Oslo University Hospital, for providing access to microscopes and for technical assistance.

Funding

This work was supported by the Norwegian Cancer Society [grant number 06039 to E.L.]; and the South-Eastern Norway Regional Health Authority [grant numbers 2008096 to A.K. and 2010017 to E.L.].

Supplementary material available online at
http://jcs.biologists.org/lookup/suppl/doi:10.1242/jcs.093500/-/DC1

References

Asamoto, M., Oyamada, M., el Aoumari, A., Gros, D. and Yamasaki, H. (1991). Molecular mechanisms of TPA-mediated inhibition of gap-junctional intercellular

communication: evidence for action on the assembly or function but not the expression of connexin 43 in rat liver epithelial cells. *Mol. Carcinog.* **4**, 322-327.

Auth, T., Schlüter, S., Urschel, S., Kussmann, P., Sonntag, S., Höher, T., Kreuzberg, M. M., Dobrowolski, R. and Willecke, K. (2009). The TSG101 protein binds to connexins and is involved in connexin degradation. *Exp. Cell Res.* **315**, 1053-1062.

Bejarano, E., Girao, H., Yuste, A., Patel, B., Marques, C., Spray, D. C., Pereira, P. and Cuervo, A. M. (2012). Autophagy modulates dynamics of connexins at the plasma membrane in a ubiquitin-dependent manner. *Mol. Biol. Cell* **23**, 2156-2169.

Bernassola, F., Karin, M., Ciechanover, A. and Melino, G. (2008). The HECT family of E3 ubiquitin ligases: multiple players in cancer development. *Cancer Cell* **14**, 10-21.

Berthoud, V. M., Rook, M. B., Traub, O., Hertzberg, E. L. and Sáez, J. C. (1993). On the mechanisms of cell uncoupling induced by a tumor promoter phorbol ester in clone 9 cells, a rat liver epithelial cell line. *Eur. J. Cell Biol.* **62**, 384-396.

Clague, M. J. and Urbé, S. (2010). Ubiquitin: same molecule, different degradation pathways. *Cell* **143**, 682-685.

El-Fouly, M. H., Trosko, J. E. and Chang, C. C. (1987). Scrape-loading and dye transfer. A rapid and simple technique to study gap junctional intercellular communication. *Exp. Cell Res.* **168**, 422-430.

Falk, M. M., Baker, S. M., Gumpert, A. M., Segretain, D. and Buckheit, R. W., 3rd (2009). Gap junction turnover is achieved by the internalization of small endocytic double-membrane vesicles. *Mol. Biol. Cell* **20**, 3342-3352.

Fallon, R. F. and Goodenough, D. A. (1981). Five-hour half-life of mouse liver gap-junction protein. *J. Cell Biol.* **90**, 521-526.

Fukuchi, M., Fukai, Y., Masuda, N., Miyazaki, T., Nakajima, M., Sohda, M., Manda, R., Tsukada, K., Kato, H. and Kuwano, H. (2002). High-level expression of the Smad ubiquitin ligase Smurf2 correlates with poor prognosis in patients with esophageal squamous cell carcinoma. *Cancer Res.* **62**, 7162-7165.

Girão, H., Catarino, S. and Pereira, P. (2009). Eps15 interacts with ubiquitinated Cx43 and mediates its internalization. *Exp. Cell Res.* **315**, 3587-3597.

Gould, G. W. and Lippincott-Schwartz, J. (2009). New roles for endosomes: from vesicular carriers to multi-purpose platforms. *Nat. Rev. Mol. Cell Biol.* **10**, 287-292.

Hesketh, G. G., Shah, M. H., Halperin, V. L., Cooke, C. A., Akar, F. G., Yen, T. E., Kass, D. A., Machamer, C. E., Van Eyk, J. E. and Tomaselli, G. F. (2010). Ultrastructure and regulation of lateralized connexin43 in the failing heart. *Circ. Res.* **106**, 1153-1163.

Ingham, R. J., Gish, G. and Pawson, T. (2004). The Nedd4 family of E3 ubiquitin ligases: functional diversity within a common modular architecture. *Oncogene* **23**, 1972-1984.

Inoue, Y. and Imamura, T. (2008). Regulation of TGF-beta family signaling by E3 ubiquitin ligases. *Cancer Sci.* **99**, 2107-2112.

Jin, C., Yang, Y. A., Anver, M. R., Morris, N., Wang, X. and Zhang, Y. E. (2009). Smad ubiquitination regulatory factor 2 promotes metastasis of breast cancer cells by enhancing migration and invasiveness. *Cancer Res.* **69**, 735-740.

Jordan, K., Solan, J. L., Dominguez, M., Sia, M., Hand, A., Lampe, P. D. and Laird, D. W. (1999). Trafficking, assembly, and function of a connexin43-green fluorescent protein chimera in live mammalian cells. *Mol. Biol. Cell* **10**, 2033-2050.

Jordan, K., Chodock, R., Hand, A. R. and Laird, D. W. (2001). The origin of annular junctions: a mechanism of gap junction internalization. *J. Cell Sci.* **114**, 763-773.

Kanemitsu, M. Y. and Lau, A. F. (1993). Epidermal growth factor stimulates the disruption of gap junctional communication and connexin43 phosphorylation independent of 12-0-tetradecanoylphorbol 13-acetate-sensitive protein kinase C: the possible involvement of mitogen-activated protein kinase. *Mol. Biol. Cell* **4**, 837-848.

Kavsak, P., Rasmussen, R. K., Causing, C. G., Bonni, S., Zhu, H., Thomsen, G. H. and Wrana, J. L. (2000). Smad7 binds to Smurf2 to form an E3 ubiquitin ligase that targets the TGF beta receptor for degradation. *Mol. Cell* **6**, 1365-1375.

King, T. J. and Lampe, P. D. (2004). The gap junction protein connexin32 is a mouse lung tumor suppressor. *Cancer Res.* **64**, 7191-7196.

Kjenseth, A., Fykerud, T., Rivedal, E. and Leithe, E. (2010). Regulation of gap junction intercellular communication by the ubiquitin system. *Cell. Signal.* **22**, 1267-1273.

Laing, J. G., Tadros, P. N., Westphale, E. M. and Beyer, E. C. (1997). Degradation of connexin43 gap junctions involves both the proteasome and the lysosome. *Exp. Cell Res.* **236**, 482-492.

Laird, D. W. (2005). Connexin phosphorylation as a regulatory event linked to gap junction internalization and degradation. *Biochim. Biophys. Acta* **1711**, 172-182.

Laird, D. W., Puranam, K. L. and Revel, J. P. (1991). Turnover and phosphorylation dynamics of connexin43 gap junction protein in cultured cardiac myocytes. *Biochem. J.* **273**, 67-72.

Lampe, P. D. (1994). Analyzing phorbol ester effects on gap junctional communication: a dramatic inhibition of assembly. *J. Cell Biol.* **127**, 1895-1905.

Lampe, P. D. and Lau, A. F. (2000). Regulation of gap junctions by phosphorylation of connexins. *Arch. Biochem. Biophys.* **384**, 205-215.

Lampe, P. D., TenBroek, E. M., Burt, J. M., Kurata, W. E., Johnson, R. G. and Lau, A. F. (2000). Phosphorylation of connexin43 on serine368 by protein kinase C regulates gap junctional communication. *J. Cell Biol.* **149**, 1503-1512.

Langlois, S., Cowan, K. N., Shao, Q., Cowan, B. J. and Laird, D. W. (2010). The tumor-suppressive function of Connexin43 in keratinocytes is mediated in part via interaction with caveolin-1. *Cancer Res.* **70**, 4222-4232.

Larsen, W. J. and Hai-Nan, (1978). Origin and fate of cytoplasmic gap junctional vesicles in rabbit granulosa cells. *Tissue Cell* **10**, 585-598.

Lauf, U., Giepmans, B. N., Lopez, P., Braconnot, S., Chen, S. C. and Falk, M. M. (2002). Dynamic trafficking and delivery of connexons to the plasma membrane and accretion to gap junctions in living cells. *Proc. Natl. Acad. Sci. USA* **99**, 10446-10451.

Leithe, E. and Rivedal, E. (2004a). Epidermal growth factor regulates ubiquitination, internalization and proteasome-dependent degradation of connexin43. *J. Cell Sci.* **117**, 1211-1220.

Leithe, E. and Rivedal, E. (2004b). Ubiquitination and down-regulation of gap junction protein connexin-43 in response to 12-O-tetradecanoylphorbol 13-acetate treatment. *J. Biol. Chem.* **279**, 50089-50096.

Leithe, E., Cruciani, V., Sanner, T., Mikalsen, S. O. and Rivedal, E. (2003). Recovery of gap junctional intercellular communication after phorbol ester treatment requires proteasomal degradation of protein kinase C. *Carcinogenesis* **24**, 1239-1245.

Leithe, E., Brech, A. and Rivedal, E. (2006a). Endocytic processing of connexin43 gap junctions: a morphological study. *Biochem. J.* **393**, 59-67.

Leithe, E., Sirnes, S., Omori, Y. and Rivedal, E. (2006b). Downregulation of gap junctions in cancer cells. *Crit. Rev. Oncog.* **12**, 225-256.

Leithe, E., Kjenseth, A., Sirnes, S., Stenmark, H., Brech, A. and Rivedal, E. (2009). Ubiquitylation of the gap junction protein connexin-43 signals its trafficking from early endosomes to lysosomes in a process mediated by Hrs and Tsg101. *J. Cell Sci.* **122**, 3883-3893.

Leithe, E., Sirnes, S., Fykerud, T., Kjenseth, A. and Rivedal, E. (2012). Endocytosis and post-endocytic sorting of connexins. *Biochim. Biophys. Acta* **1818**, 1870-1879.

Leykauf, K., Salek, M., Bomke, J., Frech, M., Lehmann, W. D., Dürst, M. and Alonso, A. (2006). Ubiquitin protein ligase Nedd4 binds to connexin43 by a phosphorylation-modulated process. *J. Cell Sci.* **119**, 3634-3642.

Lichtenstein, A., Minogue, P. J., Beyer, E. C. and Berthoud, V. M. (2011). Autophagy: a pathway that contributes to connexin degradation. *J. Cell Sci.* **124**, 910-920.

Malerød, L., Pedersen, N. M., Sem Wegner, C. E., Lobert, V. H., Leithe, E., Brech, A., Rivedal, E., Liestøl, K. and Stenmark, H. (2011). Cargo-dependent degradation of ESCRT-I as a feedback mechanism to modulate endosomal sorting. *Traffic* **12**, 1211-1226.

McLachlan, E., Shao, Q., Wang, H. L., Langlois, S. and Laird, D. W. (2006). Connexins act as tumor suppressors in three-dimensional mammary cell organoids by regulating differentiation and angiogenesis. *Cancer Res.* **66**, 9886-9894.

Mesnil, M., Crespin, S., Avanzo, J. L. and Zaidan-Dagli, M. L. (2005). Defective gap junctional intercellular communication in the carcinogenic process. *Biochim. Biophys. Acta* **1719**, 125-145.

Montesano, R., Saint Vincent, L., Drevon, C. and Tomatis, L. (1975). Production of epithelial and mesenchymal tumours with rat liver cells transformed in vitro. *Int. J. Cancer* **16**, 550-558.

Murray, S. A., Larsen, W. J., Trout, J. and Donta, S. T. (1981). Gap junction assembly and endocytosis correlated with patterns of growth in a cultured adrenocortical tumor cell (SW-13). *Cancer Res.* **41**, 4063-4074.

Musil, L. S. and Goodenough, D. A. (1991). Biochemical analysis of connexin43 intracellular transport, phosphorylation, and assembly into gap junctional plaques. *J. Cell Biol.* **115**, 1357-1374.

Naus, C. C. and Laird, D. W. (2010). Implications and challenges of connexin connections to cancer. *Nat. Rev. Cancer* **10**, 435-441.

Naus, C. C., Hearn, S., Zhu, D., Nicholson, B. J. and Shivers, R. R. (1993). Ultrastructural analysis of gap junctions in C6 glioma cells transfected with connexin43 cDNA. *Exp. Cell Res.* **206**, 72-84.

Nickel, B. M., DeFranco, B. H., Gay, V. L. and Murray, S. A. (2008). Clathrin and Cx43 gap junction plaque endoexocytosis. *Biochem. Biophys. Res. Commun.* **374**, 679-682.

Opsahl, H. and Rivedal, E. (2000). Quantitative determination of gap junction intercellular communication by scrape loading and image analysis. *Cell Adhes. Commun.* **7**, 367-375.

Osmundson, E. C., Ray, D., Moore, F. E., Gao, Q., Thomsen, G. H. and Kiyokawa, H. (2008). The HECT E3 ligase Smurf2 is required for Mad2-dependent spindle assembly checkpoint. *J. Cell Biol.* **183**, 267-277.

Osmundson, E. C., Ray, D., Moore, E. and Kiyokawa, H. (2009). Smurf2 as a novel mitotic regulator: From the spindle assembly checkpoint to tumorigenesis. *Cell Div.,* **4**, 14.

Ozdamar, B., Bose, R., Barrios-Rodiles, M., Wang, H. R., Zhang, Y. and Wrana, J. L. (2005). Regulation of the polarity protein Par6 by TGFbeta receptors controls epithelial cell plasticity. *Science* **307**, 1603-1609.

Pickart, C. M. (2001). Mechanisms underlying ubiquitination. *Annu. Rev. Biochem.* **70**, 503-533.

Piehl, M., Lehmann, C., Gumpert, A., Denizot, J. P., Segretain, D. and Falk, M. M. (2007). Internalization of large double-membrane intercellular vesicles by a clathrin-dependent endocytic process. *Mol. Biol. Cell* **18**, 337-347.

Plante, I., Stewart, M. K., Barr, K., Allan, A. L. and Laird, D. W. (2010). Cx43 suppresses mammary tumor metastasis to the lung in a Cx43 mutant mouse model of human disease. *Oncogene* **30**, 1681-1692.

Qin, H., Shao, Q., Igdoura, S. A., Alaoui-Jamali, M. A. and Laird, D. W. (2003). Lysosomal and proteasomal degradation play distinct roles in the life cycle of Cx43 in gap junctional intercellular communication-deficient and -competent breast tumor cells. *J. Biol. Chem.* **278**, 30005-30014.

Rivedal, E. and Opsahl, H. (2001). Role of PKC and MAP kinase in EGF- and TPA-induced connexin43 phosphorylation and inhibition of gap junction intercellular communication in rat liver epithelial cells. *Carcinogenesis* **22**, 1543-1550.

Rivedal, E. and Leithe, E. (2005). Connexin43 synthesis, phosphorylation, and degradation in regulation of transient inhibition of gap junction intercellular communication by the phorbol ester TPA in rat liver epithelial cells. *Exp. Cell Res.* **302**, 143-152.

Rivedal, E., Mollerup, S., Haugen, A. and Vikhamar, G. (1996). Modulation of gap junctional intercellular communication by EGF in human kidney epithelial cells. *Carcinogenesis* **17**, 2321-2328.

Ruch, R. J., Trosko, J. E. and Madhukar, B. V. (2001). Inhibition of connexin43 gap junctional intercellular communication by TPA requires ERK activation. *J. Cell. Biochem.* **83**, 163-169.

Saez, J. C., Berthoud, V. M., Branes, M. C., Martinez, A. D. and Beyer, E. C. (2003). Plasma membrane channels formed by connexins: their regulation and functions. *Physiol. Rev.* **83**, 1359-1400.

Sirnes, S., Leithe, E. and Rivedal, E. (2008). The detergent resistance of Connexin43 is lost upon TPA or EGF treatment and is an early step in gap junction endocytosis. *Biochem. Biophys. Res. Commun.* **373**, 597-601.

Sirnes, S., Kjenseth, A., Leithe, E. and Rivedal, E. (2009). Interplay between PKC and the MAP kinase pathway in Connexin43 phosphorylation and inhibition of gap junction intercellular communication. *Biochem. Biophys. Res. Commun.* **382**, 41-45.

Sirnes, S., Bruun, J., Kolberg, M., Kjenseth, A., Lind, G. E., Svindland, A., Brech, A., Nesbakken, A., Lothe, R. A., Leithe, E. et al. (2012). Connexin43 acts as a colorectal cancer tumor suppressor and predicts disease outcome. *Int. J. Cancer* **131**, 570-581.

Söhl, G. and Willecke, K. (2003). An update on connexin genes and their nomenclature in mouse and man. *Cell Commun. Adhes.* **10**, 173-180.

Solan, J. L. and Lampe, P. D. (2007). Key connexin 43 phosphorylation events regulate the gap junction life cycle. *J. Membr. Biol.* **217**, 35-41.

Solan, J. L. and Lampe, P. D. (2009). Connexin43 phosphorylation: structural changes and biological effects. *Biochem. J.* **419**, 261-272.

VanSlyke, J. K., Deschenes, S. M. and Musil, L. S. (2000). Intracellular transport, assembly, and degradation of wild-type and disease-linked mutant gap junction proteins. *Mol. Biol. Cell* **11**, 1933-1946.

Vaughan, D. K. and Lasater, E. M. (1990). Renewal of electrotonic synapses in teleost retinal horizontal cells. *J. Comp. Neurol.* **299**, 364-374.

Vaughan, D. K. and Lasater, E. M. (1992). Acid phosphatase localization in endocytosed horizontal cell gap junctions. *Vis. Neurosci.* **8**, 77-81.

Warn-Cramer, B. J., Cottrell, G. T., Burt, J. M. and Lau, A. F. (1998). Regulation of connexin-43 gap junctional intercellular communication by mitogen-activated protein kinase. *J. Biol. Chem.* **273**, 9188-9196.

Zhang, Y., Chang, C., Gehling, D. J., Hemmati-Brivanlou, A. and Derynck, R. (2001). Regulation of Smad degradation and activity by Smurf2, an E3 ubiquitin ligase. *Proc. Natl. Acad. Sci. USA* **98**, 974-979.

Zhang, Y. W., Nakayama, K., Nakayama, K. and Morita, I. (2003). A novel route for connexin 43 to inhibit cell proliferation: negative regulation of S-phase kinase-associated protein (Skp 2). *Cancer Res.* **63**, 1623-1630.

Zhu, H., Kavsak, P., Abdollah, S., Wrana, J. L. and Thomsen, G. H. (1999). A SMAD ubiquitin ligase targets the BMP pathway and affects embryonic pattern formation. *Nature* **400**, 687-693.

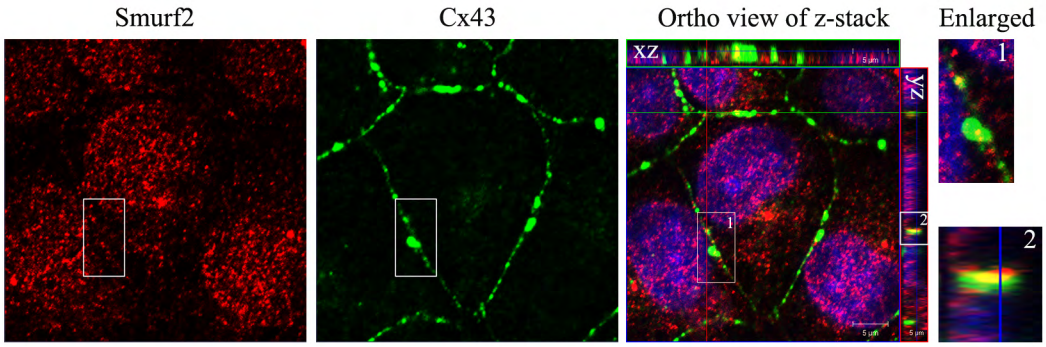

Fig. S1. Co-localization between Smurf2 and Cx43 in gap junctions in untreated cells. Cells were double-stained with anti-Cx43 and anti-Smurf2 antibodies and visualized using immunofluorescence confocal microscopy. Z-stack images were acquired at 0.38 µm intervals, and xy view as well as z-sectional views (xz and yz) are presented in the ortho view of the z-stack. Merged image is shown in the right panel, with yellow indicating co-localization between Cx43 and Smurf2. Representative Cx43 gap junctions showing co-localization with Smurf2 are presented in the enlarged images 1 (xy view) and 2 (zy view). Scale bar, 5 µm.

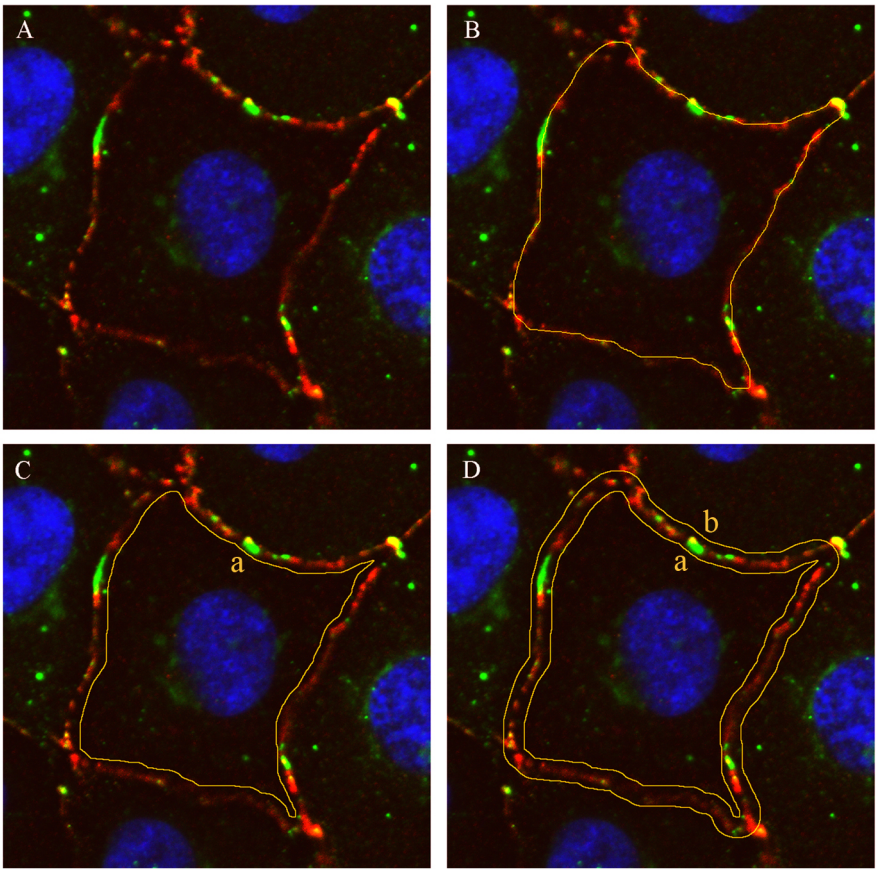

Fig. S2. Quantification of Cx43 at the plasma membrane. (**A-D**) IAR20 cells were fixed, stained with anti-Cx43 (green) and anti-occludin (red) antibodies and visualized using immunofluorescence confocal microscopy. Cx43 staining in the plasma membrane in percent of total cellular Cx43 in the same focal plane was quantified using ImageJ software as described in the 'Materials and Methods' section.